Protein Tyrosine Phosphatase 4A3 (PTP4A3) Promotes Human Uveal Melanoma Aggressiveness Through Membrane Accumulation of Matrix Metalloproteinase 14 (MMP14)

Selma Maacha,[1,2] Océane Anezo,[1,2] Malika Foy,[1,2] Géraldine Liot,[1,2] Laurence Mery,[1,2] Cécile Laurent,[3] Xavier Sastre-Garau,[4] Sophie Piperno-Neumann,[5] Nathalie Cassoux,[6] Nathalie Planque,[1,7] and Simon Saule[1,2]

[1]Institut Curie, PSL Research University, Centre National de La Recherche Scientifique (CNRS), Institut National de la Santé Et de la Recherche Médicale (INSERM), Unité Mixte de Recherche 3347 (UMR), Unité 1021 Orsay, France
[2]Université Paris Sud, Université Paris-Saclay, Centre National de La Recherche Scientifique, Unité Mixte de Recherche 3347, Unité 1021, Orsay, France
[3]Residual Tumor & Response to Treatment Lab, Institut Curie - Translational Research Department, Paris, France
[4]Tumor Biology Department, Institut Curie, Paris, France
[5]Department of Medical Oncology, Institut Curie, Paris, France
[6]Department of Surgical Oncology, Institut Curie, Paris, France
[7]Université Paris Diderot, Sorbonne Paris Cité, Paris, France

Correspondence: Simon Saule, Institut Curie, Section Recherche, Unité Mixte de Recherche 3347/ Unité 1021, Campus Universitaire d'Orsay Bâtiment 110, 91405 Orsay Cedex, France;
simon.saule@curie.fr.

Submitted: December 2, 2015
Accepted: March 11, 2016

Citation: Maacha S, Anezo O, Foy M, et al. Protein tyrosine phosphatase 4A3 (PTP4A3) promotes human uveal melanoma aggressiveness through membrane accumulation of matrix metalloproteinase 14 (MMP14). *Invest Ophthalmol Vis Sci*. 2016;57:1982–1990. DOI:10.1167/iovs.15-18780

Purpose. To study PTP4A3 phosphatase and MMP14 metalloprotease synergy in uveal melanoma aggressiveness.

Methods. Cell membrane localization of matrix metalloprotease 14 (MMP14) in uveal melanoma cells expressing protein tyrosine phosphatase A3 (PTP4A3) was assessed by flow cytometry or immunohistochemistry. The vesicular trafficking of MMP14 in the presence of PTP4A3 was evaluated in OCM-1 cells expressing either the wild-type or mutated phosphatase. Finally, MMP14 localization at the cell membrane of OCM-1 cells was impaired using RNA interference, and the PTP4A3-related migration in vitro and invasiveness in vivo of the treated cells were evaluated.

Results. We found that the membrane-anchored MMP14 is enriched at the cell surface of OCM-1 cells, patient-derived xenograft cells, and human primary uveal melanoma tumors expressing PTP4A3. Moreover, we show that PTP4A3 and MMP14 colocalize and that the vesicular trafficking of MMP14 is faster in the presence of active PTP4A3. Finally, we demonstrate that inhibition of MMP14 expression in uveal melanoma cells expressing PTP4A3 impairs their migration in vitro and invasiveness in vivo.

Conclusions. Our observations indicate that PTP4A3 increases cell membrane accumulation of MMP14 as a result of increased cellular trafficking of the metalloprotease. We also show that downregulation of MMP14 expression reduced PTP4A3-induced cell migration and invasiveness. Taken together, our findings suggest that PTP4A3-related subcellular localization of MMP14 is an important event in metastasis induction.

Keywords: metastasis, uveal melanoma, PTP4A3, MMP14

Uveal melanoma (UM) is the most common primary intraocular malignancy in adults, and constitutes 5% of all melanomas. At diagnosis, the tumor is confined to the eye in over 95% of patients, but approximately 50% subsequently develop metastases, predominantly in the liver.[1–3] Several anatomic and histologic indicators, TNM (tumor, lymph node, and metastasis) classification, and genome-wide and gene expression profiling (GEP) can be used to estimate prognosis. Gene expression profiling has identified two major subgroups of UM based on their metastatic potential; the subgroup with high metastatic potential is associated with loss of function BRCA associated protein 1 (*BAP1*) mutations.[4,5] Using this type of transcriptomic approach, we previously showed that strong expression of *PTP4A3/PRL-3* (protein tyrosine phosphatase 4A3/phosphatase of regenerating liver-3), a gene encoding a dual-specificity protein phosphatase, is predictive of metastasis occurrence.[6,7] *PTP4A3* expression in UM cells increases their migration in vitro and invasiveness in vivo.[6]

Proteolytic events at the cell surface are required for cell migration and invasiveness that occur during many physiological and pathologic processes such as tissue repair, immunity, and angiogenesis.[8,9] This localized proteolysis is performed by matrix metalloproteases (MMPs), a class of molecules that are responsible for the degradation and turnover of the extracellular matrix (ECM). Matrix metalloproteinases are a family of zinc-dependent endopeptidases that are either secreted into the

extracellular space or bound to the plasma membrane and known as membrane-type MMPs (MT-MMPs).[10,11] One of these MT-MMPs, MT1-MMP (more commonly known as matrix metalloproteinase 14 [MMP14]), plays an important role in the aggressiveness of several types of tumors, including breast cancer,[12] ovarian cancer,[13] sinonasal and oral malignant melanomas,[14] and skin melanoma.[15]

Matrix metalloproteinase 14 is produced as an inactive ~60 kDa zymogen that is activated in the trans-Golgi by furin-like convertases, which cleave the amino acid motif (RRKR) located between the propeptide and the catalytic domain.[16] The resulting activated ~57 kDa MMP14 is transported to the cell surface and tethered to the plasma membrane through a carboxyterminal transmembrane domain. At this site, active MMP14 can directly degrade a wide variety of ECM components such as collagen type I, II, and III; laminins 1 and 5; fibronectin; vitronectin; fibrin; and aggrecan. It can also indirectly process ECM components through activation of pro-MMP2.[16] Additionally, the surface proteolytic activity of MMP14 can be negatively regulated by internalization through a mechanism dependent on both clathrin- and caveolin-mediated pathways[17–19]; the internalized MMP14 can be recycled back to the plasma membrane.[20] There is increasing evidence that the regulation of MMP14 exposure at the cell surface and consequently the proteolytic activity toward ECM components are dependent upon phosphorylation of the cytoplasmic tail of MMP14 at Thr[567] as shown previously.[21] Indeed, dephosphorylation of this residue reduced internalization of MMP14.[21,22]

Since cell migration and invasiveness are both related to proteolytic events at the cell surface, we assessed the proteolytic activity at the surface of cells expressing protein tyrosine phosphatase 4A3 (PTP4A3). The proteolytic activity was mainly due to the accumulation of MMP14 at the cell surface in the presence of the PTP4A3 phosphatase, and as a consequence of enhanced overall MMP14 trafficking. Downregulation of MMP14 expression by RNA interference specifically diminished PTP4A3-related cell migration and invasiveness. Thus, our study demonstrates that MMP14 functions downstream of PTP4A3 to promote UM cell migration and invasiveness.

Methods

Cell Culture and Transfection

Human OCM-1 UM cells were obtained in 2003 from Frederic Mouriaux.[6,23] Stable OCM-1-EGFP-PTP4A3, EGFP-PTP4A3(C104S), or EGFP cell lines, previously described,[6] were maintained in DMEM-F12 (Gibco, Invitrogen, Saint Aubin, France) with 10% fetal bovine serum (FBS) (HyClone UK Laboratories, Cramlington, UK) and 1% MEM Vitamin Solution (Gibco, Invitrogen).

Human patient-derived xenograft PDX-MP55, -MP34, and -MP41 have been established and characterized from primary tumor samples as described previously.[24] Human PDX-MP41 are classified as tumors of low metastatic potential class bearing the *GNA11* mutation and wild-type *BAP1*, disomic for chromosome 3.[24] Human PDX-MP34 are of uncertain classification (more likely low/intermediate metastatic potential class) as they bear *GNA11* mutation, wild-type *BAP1*, and partial loss of chromosome 3.[24] Finally, human PDX-MP55 are classified as tumors of high metastatic potential class bearing the *GNA11* and *BAP1* mutations and are monosomic for chromosome 3.[24] Patient-derived xenograft (PDX) cells were maintained in RPMI (Gibco, Invitrogen) with 20% FBS (HyClone UK Laboratories). Stable or transient transfection was performed using Lipofectamine LTX (Invitrogen, Cergy-Pontoise, France) according to the manufacturer's instructions; 24 hours post transfection, positive cells were sorted by flow cytometry.

MISSION lentiviral transduction particles were purchased from Sigma-Aldrich (Lyon, France). OCM-1 cells were transduced with a pool of five different small hairpin RNA (shRNA) lentiviral particles, each of them encoding for a different MMP14 target-specific construct (SHCLNV, target set generated from accession number NM_004995) (Supplementary Table S1) or control nontarget shRNA (sc-108080; Santa Cruz Biotechnologies, Tebu-bio, Le Perray-en-Yvelines, France). OCM-1 cells expressing the shRNAs were selected with puromycin.

Constructs and Antibodies

The pEGFPc1 (Clontech, Mountan View, CA, USA) plasmids encoding for the wild-type form of PTP4A3 (pEGFP-PTP4A3) or the catalytic mutant (pEGFP-PTP4A3(C104S)) were both kindly provided by Qi Zeng (IMCB Institute, Singapore) and were first described by Zeng et al.[25] The MMP14-mCherry construct was kindly provided by P. Chavrier (Institut Curie, Paris, France). Rabbit monoclonal or mouse monoclonal anti-MMP14 antibodies (ab51074 and ab56307, respectively) were purchased from Abcam (Cambridge, UK), and mouse monoclonal anti-β-actin (clone AC-74) was purchased from Sigma-Aldrich. All fluorochrome-conjugated secondary antibodies were purchased from Molecular Probes (Eugene, OR, USA).

MMP14 Proteolytic Activity Assay

Matrix metalloproteinase 14 proteolytic activity was measured using the Sensolyte 520 MMP14 assay kit (Anaspec, Tebu-bio, Le Perray-en-Yvelines, France). Uveal melanoma cells were seeded on a collagen I matrix at a final concentration of 50 μg/mL (BD Biosciences, Le pont de claix, France), incubated for 24 hours, and then starved of serum for an additional 24 hours. Cells were detached using a nonenzymatic cell dissociation solution (Sigma-Aldrich), centrifuged for 4 minutes at 300*g*, and resuspended in 0.05% azide in PBS. Matrix metalloproteinase 14 substrate (5-FAM/QXL 520 FRET peptide) was diluted 1:100 in 0.05% azide in PBS, and aliquots were incubated with 10,000 cells for 50 minutes at 37°C. The samples were centrifuged and supernatants transferred to 96-well plates to measure fluorescence intensity at excitation/emission wavelengths of 490 ± 20 nm and 520 ± 20 nm, respectively.

Flow Cytometry

Uveal melanoma cells or human PDX cells were seeded on a collagen I matrix, incubated for 24 hours, serum starved for additional 24 hours, and dissociated using a nonenzymatic dissociation solution (Sigma-Aldrich). Cells were pelleted by centrifugation at 300*g* for 5 minutes and resuspended in 0.05% azide + 3% FBS in PBS. To assess the amount of MMP14 at the cell surface, nonpermeabilized cells were incubated with rabbit monoclonal anti-MMP14 antibody or the isotype control diluted 1:400 at 4°C for 1 hour. After two washes with 0.05% azide/3% FBS in PBS, the cells were incubated with anti-rabbit Alexa 647–conjugated secondary antibody (Molecular Probes) diluted 1:500 at 4°C for 1 hour, and washed twice with 0.05% azide in PBS. The cell surface MMP14 staining was analyzed using an influx cell sorting cytometer (BD Influx System, BD Biosciences).

Tumor Samples and Immunohistochemistry

Tumor samples were obtained by enucleation of untreated patients and were provided by the Biological Resource Center of the Curie Institute. The study was approved by the ethics

committee of the Curie Institute and conformed to the Declaration of Helsinki. As required by French regulations, informed consent was obtained from the patients. Matrix metalloproteinase 14 localization was investigated in a set of previously published primary human UM tumors with weak (meta0, $n = 6$) or strong (meta1, $n = 5$) PTP4A3 protein expression.[6] Tumor sections (3 μm thick) were prepared from paraffin-embedded tumor samples and processed for immunohistochemistry by an automated procedure. A monoclonal rabbit anti-MMP14 antibody (ab51074, Abcam) was used at a dilution of 1:500. Samples were counterstained with hematoxylin after immunostaining. Quantification of MMP14 localization was performed using ImageJ (https://imagej.nih.gov/ij/features.html) based on cell surface outline thresholding using the "measure" tool as a "percentage area" highlighted over total image area (across all images).

Immunofluorescence Colocalization Experiments

OCM-1 cells were rinsed with PHEM buffer (PIPES [piperazine-N,N'-bis(2-ethanesulfonic acid)] HEPES EGTA $MgCl_2$ buffer, 60, 25, 10, and 2 mM, respectively) to preserve microtubule structure and were prelysed for 3 minutes with 0.02% saponin in PHEM buffer. The cells were fixed with methanol at −20°C for 5 minutes and labeled with antibody against MMP14 (ab56307, Abcam) at a 1:500 dilution. Images were acquired using a spinning-disc confocal system (CSU-X1; Yokogawa, Roper, Evry, France) fitted on a Nikon Eclipse Ti microscope (Champigny sur Marne, France) with an oil-immersion ×63 numerical aperture (NA) 1.49 objective and an Evolve EMCCD (Photometrics, Roper, Evry, France). Pictures represent the immunostaining of a stack of two consecutive focal planes. Colocalization statistical analysis was performed under ImageJ using the JACoP plug-in.

Coimmunoprecipitation Assay

OCM-1 cells were rinsed with ice-cold PBS pH 7.4, then harvested in lysis buffer consisting of 150 mM NaCl, 50 mM Tris-HCl pH 8, 1% Nonidet P-40 (NP-40) and protease inhibitor cocktail (Sigma-Aldrich). The samples were centrifuged at 18,000*g* and 4°C to remove cellular debris, and aliquots of 1 mg total protein extract were used for the immunoprecipitation assay with the GFP-Trap kit (Chromotek, Planegg-Martinsried, Germany) according to the manufacturer's instructions.

Time-Lapse Video Microscopy and Kymograph Analyses

To assess the velocity of MMP14 vesicles, OCM-1 cells were transiently transfected with MMP14-mCherry, sorted by flow cytometry, and seeded on glass-bottom dishes (FluoroDish; World Precision Instruments, Inc., Sarasota, FL, USA) coated with collagen I (BD Biosciences) at a density of 2×10^4. The cells were starved of serum for 24 hours, and MMP14 vesicles were monitored by time-lapse video microscopy using an inverted phase-contrast microscope (Leica DMI6000B, Roper) equipped with a temperature- and CO_2-controllable environmental chamber, 1.4 NA oil-immersion ×100 objective, and an Evolve EMCCD (Photometrics, Roper). Images were acquired every 0.5 seconds for 2 minutes using Metamorph software (Molecular Devices, Saint Grégoire, France). Movies were reconstructed with a plug-in for the ImageJ software (http://rsbweb.nih.gov/ij/ [in the public domain]) developed by F. Cordelière at Institut Curie (Orsay, France). ImageJ was used to generate kymographs from time-lapse live imaging movies imported as an image stack and analyzed using the KymoToolBox plug-in ($n_{cells} \sim 13$ and $n_{vesicles/cell} \sim 70$ per each cell line).

To assess the migration velocity of the OCM-1 cells on collagen I, cells were monitored by time-lapse video microscopy as previously described[6] ($n = 50$ cells per each cell line).

Chorioallantoic Membrane (CAM) Assay

Fertilized chick eggs (EARL Morizeau, Dangers, France) were incubated at 38°C with 80% humidity for 8 days. Then, aliquots of 0.25×10^6 cultured melanoma cells (OCM-1-EGFP-PTP4A3 shMMP14 or OCM-1-EGFP-PTP4A3 shCtrl) were used to inoculate the CAM and the eggs incubated for 8 additional days to allow the cells to disseminate. Quantification of the relative invasiveness of OCM-1 cells in the chick femurs was based on the presence of human DNA (human *alu* sequences) within the chick femur DNA and was assessed using the $2^{\Delta\Delta CT}$ method, where $\Delta CT = CT_{alu} - CT_{GAPDH}$ and $\Delta\Delta CT = \Delta CT_{sampleofinterest} - \Delta CT_{calibrator}$. The calibrator represents noninjected chick embryos and reflects the background of the experiment. The calibrator $2^{\Delta\Delta CT}$ values were arbitrarily assigned a value of 1.

Statistical Analysis

Data are presented as means ± SD for each condition. Statistical analyses were performed using StatView software (SAS Institute, Inc., Cary, NC, USA). The Mann-Whitney test was used for comparisons.

Results

PTP4A3 Expression Promotes Localization of MMP14 at the Cell Surface

Since PTP4A3 is artificially induced in OCM-1 cells, we compared the level of PTP4A3 in these cells to PDX tumor samples. EGFP-PTP4A3 or EGFP-PTP4A3(C104S) displayed equivalent amounts of PTP4A3 protein compared to PDX-MP55, a bad prognosis tumor.[24] As expected, PDX-MP34, wild-type for *BAP1*,[24] expressed lower levels of PTP4A3 (Fig. 1A).

Invasion requires proteolysis of ECM components, and activation of MMP14 is a key event in cancer invasion.[26] To test if PTP4A3-dependent invasion is linked to MMP14, we used Western blotting to assay total MMP14 in OCM-1 UM cells expressing PTP4A3 or a catalytically inactive mutant of the phosphatase PTP4A3(C104S). The abundance of MMP14 did not appear to differ between these cells (Fig. 1B) that expressed similar levels of PTP4A3 (Supplementary Fig. S1). However, MMP14-related invasion is associated with its localization at the cell surface, so we studied endogenous MMP14 membrane localization in nonpermeabilized OCM-1 cells in the presence of PTP4A3 by flow cytometry using a specific anti-MMP14 antibody. We found that EGFP-PTP4A3–expressing cells displayed a stronger surface immunofluorescence signal than EGFP-PTP4A3(C104S) in OCM-1 cells (Figs. 1C, 1E). Using flow cytometry, surface localization of endogenous MMP14 in either EGFP-PTP4A3 or EGFP-PTP4A3(C104S) was compared to PDX-MP55 cells, which express PTP4A3 endogenously. Similar higher levels of membrane-bound MMP14 were observed in PDX-MP55 and EGFP-PTP4A3 when compared to EGFP-PTP4A3(C104S) (Fig. 1D). To demonstrate that membrane-bound MMP14 is increased in primary UM cells overexpressing PTP4A3 as shown in OCM-1 cells, PDX-MP41 (good prognosis tumor[24])

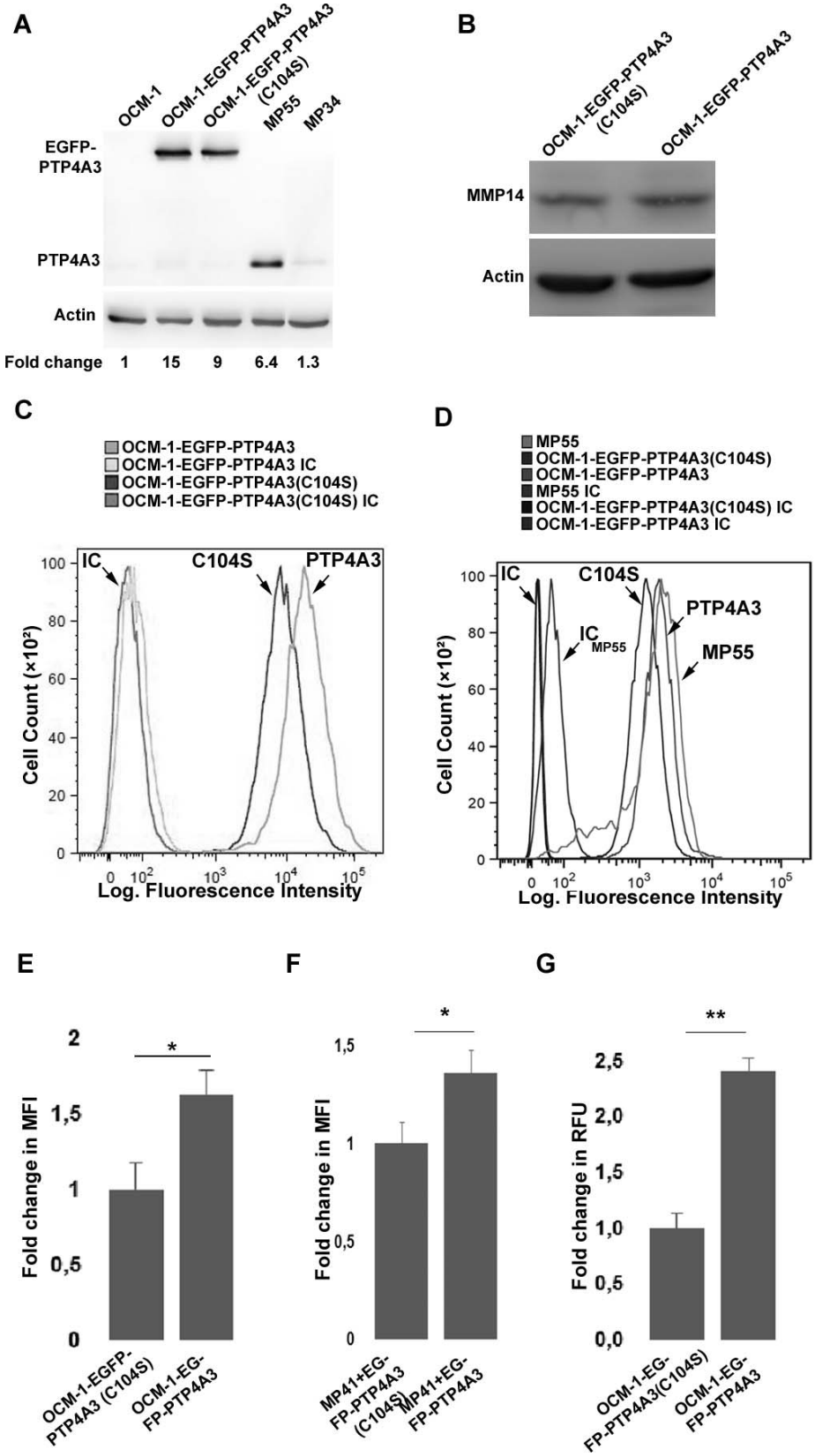

Figure 1. More MMP14 is exposed on the cell surface of UM cells in the presence of active PTP4A3. (**A**) Western blot analysis of PTP4A3 in total lysates of OCM-1, OCM-1 cells expressing EGFP-PTP4A3 or EGFP-PTP4A3(C104S), or PDX tumor samples. Fold change indicates densitometric quantification of PTP4A3 bands normalized to β-actin signal and compared to OCM-1 endogenous PTP4A3, which was arbitrarily assigned a value of 1. (**B**) Western blot analysis of MMP14 in total lysates of OCM-1 cells expressing EGFP-PTP4A3 or EGFP-PTP4A3(C104S). (**C**) MMP14 localization on the cell surface as assessed by flow cytometry in nonpermeabilized OCM-1 cells stained with primary anti-MMP14 antibody and secondary Alexa Fluor 647–conjugated antibody to label membrane-associated MMP14. (**D**) Comparison of MMP14 localization on the cell surface in

nonpermeabilized OCM-1-EGFP-PTP4A3, -EGFP-PTP4A3(C104S), and PDX-MP55 using analogous flow cytometry experiment conditions. (**E**) Quantification of surface-labeling fluorescence intensities of MMP14 based on Alexa Fluor 647 fluorescence in three independent experiments (3 × 10,000 cells). Values for EGFP-PTP4A3(C104S) were arbitrarily defined as 1. Graphs show mean ± SD. $^{*}P < 0.05$. (**F**) Cell surface MMP14 localization as assessed by flow cytometry in nonpermeablized PDX-MP41 cells transiently transfected with EGFP-PTP4A3 or EGFP-PTP4A3(C104S) encoding vectors (see Supplementary Fig. S2) and stained with MMP14 primary antibody and secondary Alexa Fluor 647–conjugated antibody to label membrane-associated MMP14. Quantification of Alexa Fluor 647 surface labeling fluorescence intensities of MMP14 from two independent experiments (2 × 5000 cells). Values of MMP14 for EGFP-PTP4A3(C104S) were arbitrarily defined as 1. Graphs show means ± SD. $^{*}P < 0.05$. (**G**) The Sensolyte 520 MMP14 assay kit was used to assay MMP14 proteolytic activity at the cell surface of nonpermeabilized OCM-1 cells expressing EGFP-PTP4A3 or EGFP-PTP4A3(C104S). Graphs show means ± SD. Each data point represents the means from three independent experiments. $^{**}P < 0.01$. IC, isotype control; MFI, mean fluorescence intensity; RFU, relative fluorescence intensity.

cells were transiently transfected with DNA vectors encoding EGFP-PTP4A3 or EGFP-PTP4A3(C104S). Since heterogeneous expression of EGFP-PTP4A3 was obtained in the transiently PDX-MP41 transfected cells, MMP14 signal was analyzed by flow cytometry in cells expressing similar EGFP levels (Supplementary Fig. S2). EGFP-PTP4A3–expressing cells displayed a stronger surface immunofluorescence signal than EGFP-PTP4A3(C104S) in PDX-MP41 cells, indicating that the amount of MMP14 at the cell surface is higher on EGFP-PTP4A3–expressing cells (Fig. 1F). Then we assayed the proteolytic activity at the cell surface of nonpermeabilized OCM-1 cells in the presence of the PTP4A3 phosphatase using the Sensolyte 520 MMP14 assay. PTP4A3-expressing cells displayed a greater surface proteolytic activity than the EGFP-PTP4A3(C104S) control cells (Fig. 1G).

PTP4A3 Accumulation Correlates With the Localization of MMP14 to the Cell Surface in Human Primary UM Tumors

In order to determine whether MMP14 membrane localization in the presence of PTP4A3 in the cell lines OCM-1 and PDX-MP41 or -MP55 was also observed in human UM samples, we performed immunohistochemistry to investigate MMP14 localization in a published set of human primary UM tumors displaying strong (meta1) or weak (meta0) PTP4A3 accumulation.[6] In the tumor sections with strong PTP4A3 accumulation, MMP14 staining displayed a clear overall cell outline expression pattern (Figs. 2a, 2a', 2c), whereas tumors sections with weak PTP4A3 expression show a more diffuse cytoplasmic pattern (Figs. 2b, 2b', 2c), suggesting that more MMP14 is localized at the cell surface in human primary UM tumors in which PTP4A3 is abundant. Quantification of the pixel intensity at the cell surface using ImageJ shows a significant increase in MMP14 localization at the cell membrane in meta1 tumors (Fig. 2d). Association between MMP14 localization and standard features of UM is shown in Supplementary Table S2.

PTP4A3 and MMP14 Colocalize and Interact

Since PTP4A3 is present at the cell membrane, we conducted immunofluorescence colocalization experiments in UM OCM-1 cells expressing EGFP-PTP4A3 to determine whether the two proteins colocalize at the plasma membrane. In fixed cells, colocalization studies of EGFP-PTP4A3 and endogenous MMP14 stained with a specific antibody revealed colocalization of the two proteins at the plasma membrane (Fig. 3A, merge). Moreover, application of Van Steensel's cross-correlation

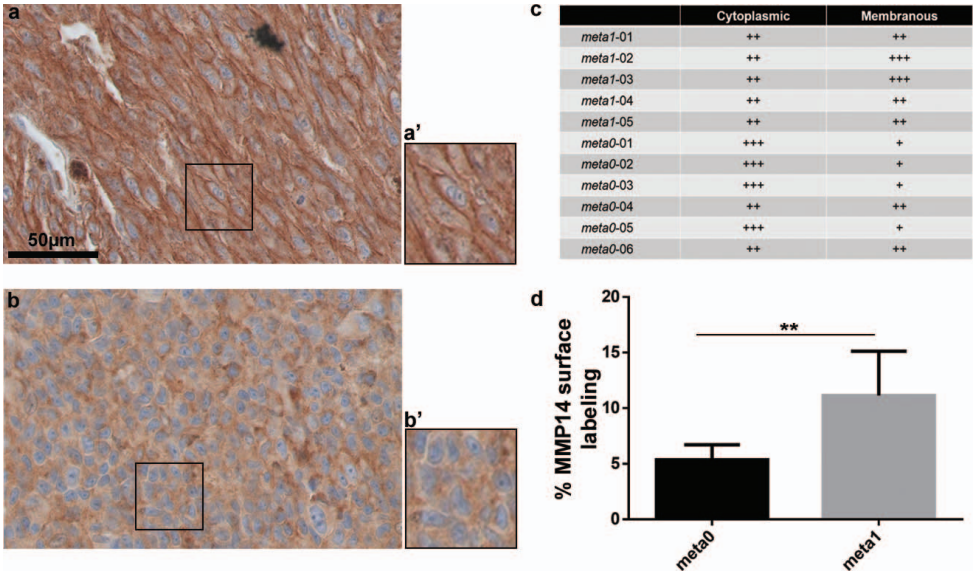

	Cytoplasmic	Membranous
meta1-01	++	++
meta1-02	++	+++
meta1-03	++	+++
meta1-04	++	++
meta1-05	++	++
meta0-01	+++	+
meta0-02	+++	+
meta0-03	+++	+
meta0-04	++	++
meta0-05	+++	+
meta0-06	++	++

FIGURE 2. MMP14 localization at the cell surface in human primary UM tumors overexpressing PTP4A3. Representative immunohistochemistry of MMP14 in meta1-03 tumors (**a**) (strong PTP4A3 staining) and meta0-05 tumors (**b**) (weak PTP4A3 staining).[6] (**a', b'**) Representations of zoom images of the rectangle zone in (**a**) and (**b**), respectively. Positive staining appears in *brown*, and nuclei were counterstained with hematoxylin (original magnification ×200). (**c**) Summary of the MMP14 staining localization at the cell membrane or in the cytoplasm of meta1 and meta0 tumors classified according to three levels: weak (+), moderate (++), or strong (+++). (**d**) Quantification of MMP14 localization at the cell surface of meta0 and meta1 tumors using ImageJ based on cell surface outline thresholding. Histograms represent the pixel intensity within the outlined cell surface. $^{**}P < 0.01$.

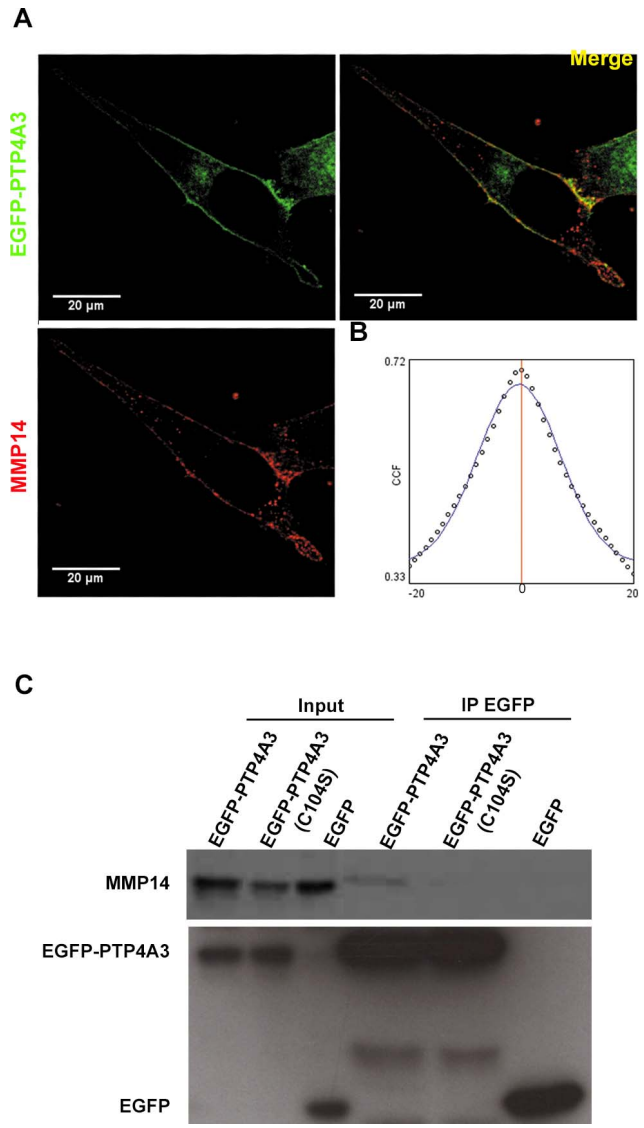

Figure 3. Colocalization and interaction of PTP4A3 and MMP14 at the cell surface. (**A**) Spinning-disc confocal microscopy of OCM-1 cells expressing EGFP-PTP4A3. Single-channel images of EGFP-PTP4A3 (*green*) and MMP14 based on Alexa Fluor 647 fluorescence (*red*) are shown in the *left column*. Merged images are shown in the *right column*. (**B**) Colocalization statistical analysis based on Van Steensel's cross-correlation function (CCF) showing positive colocalization, Pearson's coefficient = 0.725. (**C**) Total lysates of cells expressing EGFP-PTP4A3, EGFP-PTP4A3(C104S), or EGFP were subjected to coimmunoprecipitation assay using the GFP-Trap assay kit. The input consisted of 1/50th of each total lysate.

function (CCF) showed positive colocalization with a Pearson's coefficient of 0.725 (Fig. 3B). We then performed coimmunoprecipitation assays using the GFP-Trap kit to test whether MMP14 and PTP4A3 interact. Total lysates were prepared from OCM-1 cells expressing EGFP-PTP4A3, EGFP-PTP4A3(C104S), or EGFP and GFP-Trap beads used for precipitations. The input and precipitated proteins were then separated by SDS-PAGE, transferred to Polyvinylidene difluoride, and probed with anti-GFP and anti-MMP14 antibodies. MMP14 and PTP4A3 coprecipitated, indicating that they are in a complex, whereas MMP14 was much less tightly bound to the C104S mutant of PTP4A3 (Fig. 3C).

PTP4A3 Enhances MMP14 Vesicular Trafficking

The enrichment of MMP14 at the cell surface of PTP4A3-expressing cells could be the consequence of faster overall MMP14 trafficking and/or reduced endocytosis in these cells. To study the dynamics of MMP14 trafficking, OCM-1 cells were transfected with MMP14-mCherry plasmid and analyzed by time-lapse video microscopy. MMP14-mCherry was found in vesicle-like structures in the cytoplasm with pronounced accumulation in the perinuclear region and in the cell periphery of migrating cells (Fig. 4A), consistent with a previous description.[27] Kymograph analysis showed that the overall MMP14-mCherry–vesicle movement was faster in the EGFP-PTP4A3–expressing cells than EGFP-PTP4A3(C104S)– or EGFP-expressing cells (Fig. 4B, Supplementary Movie S1).

MMP14 Expression Is Required Downstream of PTP4A3 to Enhance Cell Migration and Invasiveness

We performed RNA interference experiments to determine if MMP14 function is required for the PTP4A3-related promigratory and invasive phenotypes in UM cells. Recombinant lentiviruses delivering shRNA directed against MMP14 or control nontarget shRNA were used to infect the different OCM-1 cells, and a strong reduction of MMP14 expression was confirmed by Western blotting (Fig. 5A). This inhibition of MMP14 production in OCM-1 cells was associated with decreased MMP14 localization at the cell surface (data not shown). Random cell migration on collagen I and invasiveness using the CAM in vivo dissemination assay were tested: The downregulation of MMP14 expression significantly impaired the migration velocity of EGFP-PTP4A3–expressing cells, while the migration velocity of the control cells expressing EGFP-PTP4A3(C104S) or EGFP was not affected (Fig. 5B). Similarly, downregulation of MMP14 expression decreased the PTP4A3-related invasiveness in vivo (Fig. 5C). These findings support the hypothesis that MMP14 expression is required for PTP4A3-related migration in vitro and invasiveness in vivo of OCM-1 UM cells.

Discussion

The expression of the survival-predictive gene *PTP4A3* is upregulated in UM primary tumors of bad prognosis and is strongly associated with the occurrence of metastasis. Uveal melanoma cells overexpressing PTP4A3 migrate faster in vitro and are more invasive in vivo than cells expressing the catalytically inactive mutant PTP4A3(C104S), potentially implicating PTP4A3 in the regulation of protease-encoding genes. Matrix metalloproteinase 14 is a membrane-anchored metalloprotease that plays a central role in ECM remodeling and invasion.[28,29] However, MMP14 RNA is not differentially expressed between the primary tumors of good and bad prognosis (Supplementary Fig. S3). As *PTP4A3* encodes a phosphatase, we hypothesized that it may regulate MMP14 posttranslationally. We demonstrate here that there is more MMP14 at the cell surface of UM cells expressing PTP4A3 than those expressing PTP4A3(C104S) mutant, suggesting that membrane accumulation of MMP14 is dependent on the phosphatase activity of PTP4A3. Coimmunoprecipitation experiments showed that PTP4A3 and MMP14 form a complex, and this interaction seems to be dependent on the phosphatase activity of PTP4A3: The interaction between the mutant PTP4A3(C104S) and MMP14 was barely detectable, suggesting a requirement for a functional catalytic site for the

Investigative Ophthalmology & Visual Science

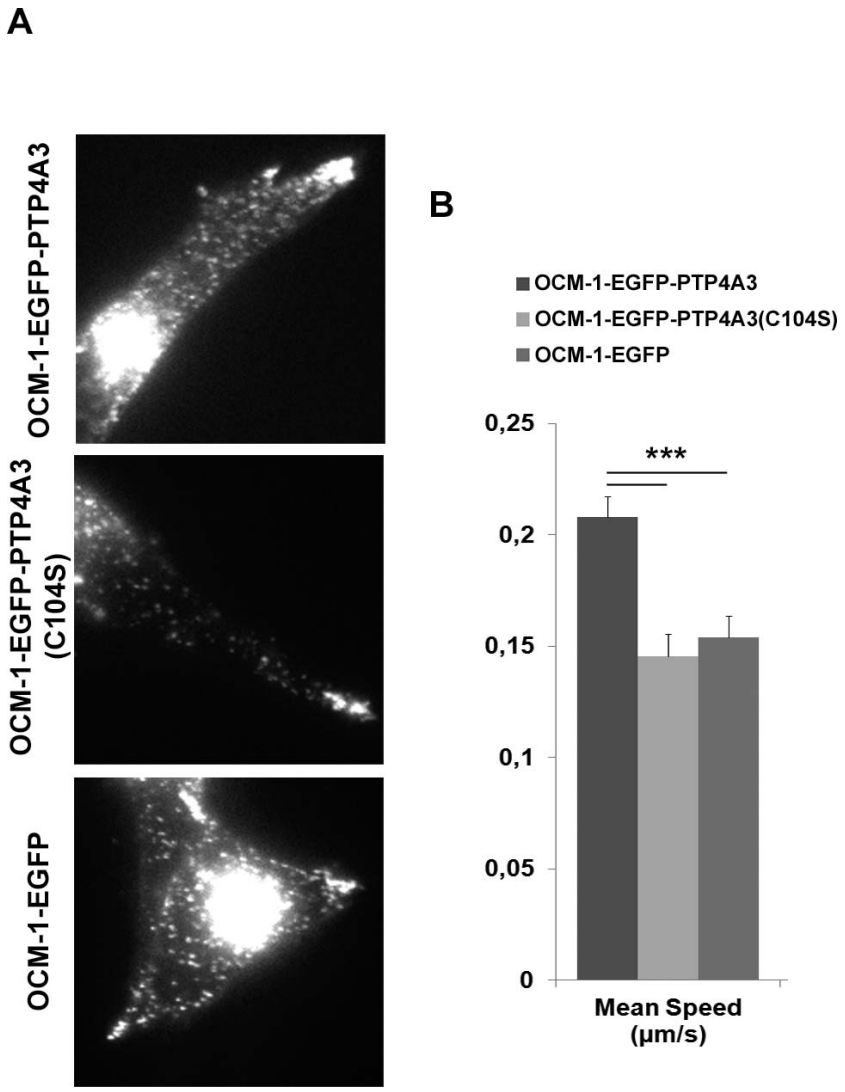

FIGURE 4. MMP14 vesicular trafficking is enhanced in the presence of PTP4A3. (**A**) Representative images revealing the vesicular localization of MMP14 in OCM-1 cells expressing EGFP-PTP4A3, EGFP-PTP4A3(C104S), or EGFP. (**B**) Kymograph quantification analysis of MMP14 vesicle migration velocity in OCM-1 cells expressing EGFP-PTP4A3, EGFP-PTP4A3(C104S), or EGFP (see also Supplementary Movie S1). Each data point represents the means from two independent experiments. Similar results were obtained in three independent experiments. $^{***}P < 0.001$.

interaction. Thus, MMP14 accumulation at the cell surface could explain the PTP4A3-related invasive phenotype in UM cells. The clinical relevance of these observations was confirmed by studying human primary UM tumors. We found that, as in OCM-1 or PDX-MP55 cells, more MMP14 was localized at the cell surface of the UM tumors overexpressing PTP4A3 than of tumors only weakly expressing PTP4A3. Cytoplasmic and cell membrane localization of MMP14 have been already reported in UM tumors, particularly in epithelioid cells, which represent a marker of bad prognosis.[30] In addition, an increase in both PTP4A3 and MMP14 expression was reported in other solid tumors such as colon cancer and gliomas.[31,32] Similar to what we observed, downregulation of MMP14 reduced the invasive properties of colon cancer cells.[31]

Thus, PTP4A3 may regulate MMP14 trafficking and/or activity by regulating its phosphorylation/dephosphorylation dynamics. There are three residues in the carboxyterminal region of MMP14 that could be processed by the PTP4A3 phosphatase: Thr^{567}, Tyr^{573}, and Ser^{578}. Dephosphorylation of these residues could modify the affinity of MMP14 for the trafficking machinery, leading to the inhibition of MMP14 internalization from the plasma membrane. It has been reported that the regulation of MMP14 exposure at the cell surface and consequently the proteolytic activity toward ECM components are dependent upon the phosphorylation of the Thr^{567} residue in the cytoplasmic tail of MMP14. Indeed, dephosphorylation of this residue reduces the internalization of MMP14.[22,21] The overall vesicular trafficking dynamics of MMP14 vesicles is faster in the OCM-1 UM cells accumulating PTP4A3 than in those expressing the mutant phosphatase. This latter observation may explain the cell membrane accumulation of MMP14 in the presence of PTP4A3. We have shown that inhibition of MMP14 expression in UM OCM-1 cells expressing PTP4A3 impairs cell migration in vitro and invasiveness in vivo, suggesting that PTP4A3 acts upstream of MMP14 to induce promigratory and invasive phenotypes.

Acknowledgments

The authors thank Lucile Chervaux, Marie-Noëlle Soler, Charlène Lasgi, and André Nicolas for their technical advice and support.

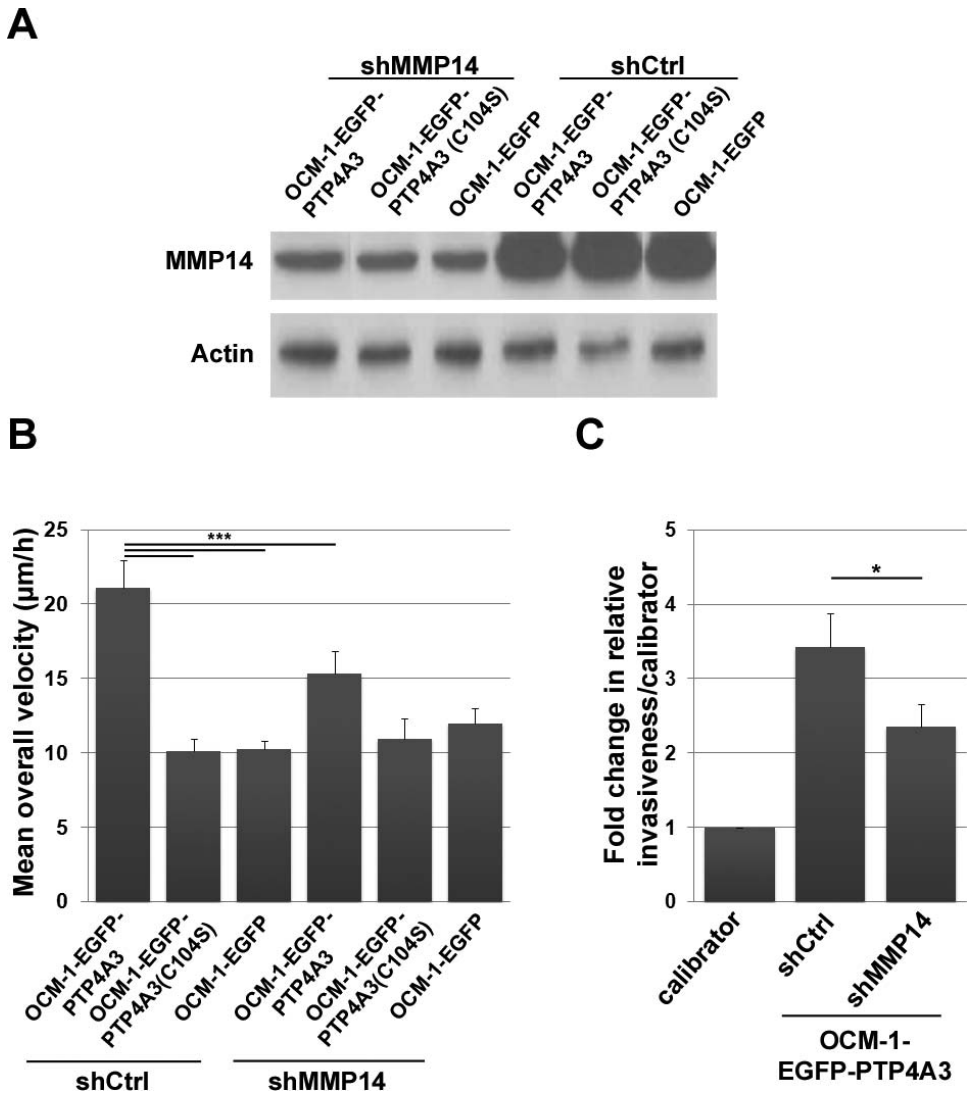

Figure 5. Involvement of MMP14 downstream of PTP4A3 in UM cell migration and invasiveness. (**A**) Western blot analysis of MMP14 showing effective downregulation of MMP14 protein production after lentiviral transduction of a set of five MMP14 target shRNAs. (**B**) The migration velocity of OCM-1 cells expressing EGFP-PTP4A3, EGFP-PTP4A3(C104S), and EGFP shCtrl or shMMP14 was measured by live videomicroscopy in a collagen I matrix. Graphs show means ± SD. Each data point represents the mean from two independent experiments. $^{***}P < 0.001$ ($n = 50$). (**C**) Quantitative analysis of the relative invasiveness of EGFP-PTP4A3 shCtrl– or shMMP14-expressing cells. Aliquots of 0.25×10^6 cells were inoculated into the CAM of chick embryos, and the presence of human cells was assessed by real-time PCR analysis of chick GAPDH and human *alu* sequences within the chick femur DNA using the $2^{\Delta\Delta CT}$ method. Values for the calibrator were arbitrarily defined as 1. Graphs show means ± SD. Each data point represents the mean for two independent experiments. $^{*}P < 0.05$ ($n_{embryos} = 14$/cell line).

Supported by grants from Retina France, Fondation de France (No. 2013 00039338), and the Programme Incitatif et Coopératif (PIC) Uveal Melanoma from the Institut Curie.

Disclosure: **S. Maacha**, None; **O. Anezo**, None; **M. Foy**, None; **G. Liot**, None; **L. Mery**, None; **C. Laurent**, None; **X. Sastre-Garau**, None; **S. Piperno-Neumann**, None; **N. Cassoux**, None; **N. Planque**, None; **S. Saule**, None

References

1. Collaborative Ocular Melanoma Study Group. Assessment of metastatic disease status at death in 435 patients with large choroidal melanoma in the Collaborative Ocular Melanoma Study (COMS): COMS report no. 15. *Arch Ophthalmol*. 2001; 119:670–676.
2. Singh AD, Topham A. Incidence of uveal melanoma in the United States: 1973-1997. *Ophthalmology*. 2003;110:956–961.
3. Singh AD, Topham A. Survival rates with uveal melanoma in the United States: 1973-1997. *Ophthalmology*. 2003;110:962–965.
4. Cassoux N, Rodrigues MJ, Plancher C, et al. Genome-wide profiling is a clinically relevant and affordable prognostic test in posterior uveal melanoma. *Br J Ophthalmol*. 2014;98:769–774.
5. Harbour JW, Onken MD, Roberson ED, et al. Frequent mutation of BAP1 in metastasizing uveal melanomas. *Science*. 2010;330:1410–1413.
6. Laurent C, Valet F, Planque N, et al. High PTP4A3 phosphatase expression correlates with metastatic risk in uveal melanoma patients. *Cancer Res*. 2011;71:666–674.
7. Matter WF, Estridge T, Zhang C, et al. Role of PRL-3, a human muscle-specific tyrosine phosphatase, in angiotensin-II signaling. *Biochem Biophys Res Commun*. 2001;283:1061–1068.

8. Gill SE, Parks WC. Metalloproteinases and their inhibitors: regulators of wound healing. *Int J Biochem Cell Biol*. 2008;40: 1334–1347.
9. Gill SE, Kassim SY, Birkland TP, Parks WC. Mouse models of MMP and TIMP function. *Methods Mol Biol*. 2010;622:31–52.
10. Deryugina EI, Quigley JP. Matrix metalloproteinases and tumor metastasis. *Cancer Metastasis Rev*. 2006;25:9–34.
11. Linder S, Wiesner C, Himmel M. Degrading devices: invadosomes in proteolytic cell invasion. *Annu Rev Cell Dev Biol*. 2011;27:185–211.
12. Yao G, He P, Chen L, Hu X, Gu F, Ye C. MT1-MMP in breast cancer: induction of VEGF-C correlates with metastasis and poor prognosis. *Cancer Cell Int*. 2013;13:98.
13. Kaimal R, Aljumaily R, Tressel SL, et al. Selective blockade of matrix metalloprotease-14 with a monoclonal antibody abrogates invasion, angiogenesis, and tumor growth in ovarian cancer. *Cancer Res*. 2013;73:2457–2467.
14. Kondratiev S, Gnepp DR, Yakirevich E, et al. Expression and prognostic role of MMP2, MMP9, MMP13, and MMP14 matrix metalloproteinases in sinonasal and oral malignant melanomas. *Hum Pathol*. 2008;39:337–343.
15. Hofmann UB, Westphal JR, Van Muijen GN, Ruiter DJ. Matrix metalloproteinases in human melanoma. *J Invest Dermatol*. 2000;115:337–344.
16. Itoh Y. MT1-MMP: a key regulator of cell migration in tissue. *IUBMB Life*. 2006;58:589–596.
17. Toth M, Hernandez-Barrantes S, Osenkowski P, et al. Complex pattern of membrane type 1 matrix metalloproteinase shedding. Regulation by autocatalytic cells surface inactivation of active enzyme. *J Biol Chem*. 2002;277:26340–36350.
18. Gálvez BG, Matías-Román S, Yáñez-Mó M, Vicente-Manzanares M, Sánchez-Madrid F, Arroyo AG. Caveolae are a novel pathway for membrane-type 1 matrix metalloproteinase traffic in human endothelial cells. *Mol Biol Cell*. 2004;15:678–687.
19. Remacle A, Murphy G, Roghi C. Membrane type I-matrix metalloproteinase (MT1-MMP) is internalised by two different pathways and is recycled to the cell surface. *J Cell Sci*. 2003; 116:3905–3916.
20. Wang X, Ma D, Keski-Oja J, Pei D. Co-recycling of MT1-MMP and MT3-MMP through the trans-Golgi network. Identification of DKV582 as a recycling signal. *J Biol Chem*. 2004;279:9331–9336.
21. Williams KC, Coppolino MG. Phosphorylation of membrane type 1-matrix metalloproteinase (MT1-MMP) and its vesicle-associated membrane protein 7 (VAMP7)-dependent trafficking facilitate cell invasion and migration. *J Biol Chem*. 2011; 286:43405–43416.
22. Moss NM, Wu YI, Liu Y, Munshi HG, Stack MS. Modulation of the membrane type 1 matrix metalloproteinase cytoplasmic tail enhances tumor cell invasion and proliferation in three-dimensional collagen matrices. *J Biol Chem*. 2009;284:19791–19799.
23. Kan-Mitchell J, Mitchell MS, Rao N, Liggett PE. Characterization of uveal melanoma cell lines that grow as xenografts in rabbit eyes. *Invest Ophthalmol Vis Sci*. 1989;30:829–834.
24. Laurent C, Gentien D, Piperno-Neumann S, et al. Patient-derived xenografts recapitulate molecular features of human uveal melanomas. *Mol Oncol*. 2013;7:625–636.
25. Zeng Q, Dong JM, Guo K, et al. PRL-3 and PRL-1 promote cell migration, invasion, and metastasis. *Cancer Res*. 2003;63: 2716–2722.
26. Barbolina MV, Stack MS. Membrane type 1-matrix metalloproteinase: substrate diversity in pericellular proteolysis. *Semin Cell Dev Biol*. 2008;19:24–33.
27. Wiesner C, Faix J, Himmel M, Bentzien F, Linder S. KIF5B and KIF3A/KIF3B kinesins drive MT1-MMP surface exposure, CD44 shedding, and extracellular matrix degradation in primary macrophages. *Blood*. 2010;116:1559–1569.
28. Friedl P, Wolf K. Proteolytic interstitial cell migration: a five-step process. *Cancer Metastasis Rev*. 2009;28:129–135.
29. Poincloux R, Lizárraga F, Chavrier P. Matrix invasion by tumour cells: a focus on MT1-MMP trafficking to invadopodia. *J Cell Sci*. 2009;122:3015–3024.
30. Lai K, Conway RM, Crouch R, Jager MJ, Madigan MC. Expression and distribution of MMPs and TIMPs in human uveal melanoma. *Exp Eye Res*. 2008;86:936–941.
31. Lee SY, Han YM, Yun J, et al. Phosphatase of regenerating liver-3 promotes migration and invasion by upregulating matrix metalloproteinases-7 in human colorectal cancer cells. *Int J Cancer*. 2012;131:E190–E203.
32. Kong L, Li Q, Wang L, Liu Z, Sun T. The value and correlation between PRL-3 expression and matrix metalloproteinase activity and expression in human gliomas. *Neuropathology*. 2007;27:516–521.

Investigative Ophthalmology & Visual Science